Analytical modelling of the transient response of thermopile-based MEMS sensors

D.V. Randjelović, A.G. Kozlov, O.M. Jakšić, M.M. Smiljanić and P.D. Poljak

***Abstract*—This work presents an analytical model dedicated to study of the transient response of multipurpose MEMS devices based on thermopile sensors. In general, thermopile sensors response depends on ambient temperature, thermal conductivity of the gas inside the housing and the pressure of the gas. The presented model takes into account all these parameters. This model was sucessfully implemented for the study of transient behaviour of our multifunctional sensors with p+Si/Al thermocouples and a bulk micromachined bilayered membrane. Simulations were performed for different gases of interest and conclusions were deduced regarding the influence of relevant parameters on the thermal time constant. This analytical approach is general and flexible enough to be implemented for analysis of the transient behaviour of thermopile-based sensors when used for different applications.**

***Index Terms*— analytical modelling, MEMS sensors, thermopile, transient response**

Original Research Paper
DOI: 10.7251/ELS1519070R

I. Introduction

Thermopile-based MEMS sensors belong to thermal type sensors with a broad range of applications (IC sensors, thermal converters, accelerometers, flow sensors, vacuum sensors, gas type sensors, chemical sensors …) [1-6]. Their performance depends on processes of heat transfer on the chip as well as on the thermal interaction between the sensor and the surrounding ambient.

We developed multifunctional sensors with p^+Si/Al thermocouples and p^+Si (P-type) or Al (A-type) heater which were succesfully tested as flow sensors, vacuum sensors and thermal converters [4-6]. The thermal isolating structure is a bilayer membrane consisting of sputtered silicon dioxide and a residual n-Si layer.

Manuscript received 30 October 2015. Received in revised form 20 October 2011.

This work has been partially supported by the Serbian Ministry of Education, Science and Technological Development within the framework of the Project TR32008.

D.V. Randjelović, O.M. Jakšić, M.M. Smiljanić and P.D. Poljak are with the Centre of Microelectronic Technologies, Institute of Chemistry, Technology and Metallurgy, University of Belgrade, Njegoševa 12, 11000 Belgrade, Serbia, (corresponding author to provide phone: +381-11-2628-587; fax: +381-11-2182-995; e-mail: danijela@nanosys.ihtm.bg.ac.rs).

A.G. Kozlov is with Omsk State University, Pr. Mira, 55a, Omsk, 644077, Russia

The performance of these sensors is strongly influenced by residual n-Si thickness. Apart from this parameter, thermopile sensors response depends on the ambient temperature, the thermal conductivity of the gas inside the housing and the pressure of the gas. This work presents an analytical model which takes into account all the relevant parameters mentioned above and is dedicated to study of transient response of multipurpose devices based on thermopile sensors.

II. Analytical Modeling of Transient Response

Based on the core analytical model introduced in [4], several special models were developed with the purpose of studying multipurpose sensor performance when the device is used for a specific application [5, 6]. The same situation is with the model described in this work. In the first part of this section the structure of A- and P-type thermopile based MEMS sensors is given, and in the second part, analytical model dedicated for study of transient response of these sensors is presented.

A. Sensor structure

Figure 1 shows a structure of a P-type sensor with a p^+Si heater mounted on a TO-8 housing. Two independent thermopiles with 30 thermocouples each are placed on a sandwich membrane consisting of sputtered silicon dioxide (1 μm) and a residual n-Si layer. A-type structures have the same design, the only difference is that their heater is formed of sputtered Al placed on the upper side of the membrane. Functional structures with residual layer thicknesses ($d_{\text{n-Si}}$) in the range (3 - 25) μm were fabricated.

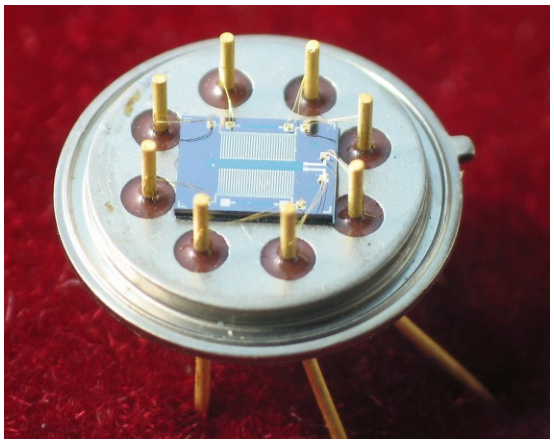

Fig. 1. P-type sensor mounted on TO-8 housing.

Figure 2 depicts the cross section of the structure along the shorter side of the chip. The lengths of the two zones used in analytical modelling are also shown. The zone 0 with the length l_0 is delimited by the middle of the chip and the outer edge of the heater. The zone 1 with the length l_1 is delimited by the outer edge of the heater and the membrane edge.

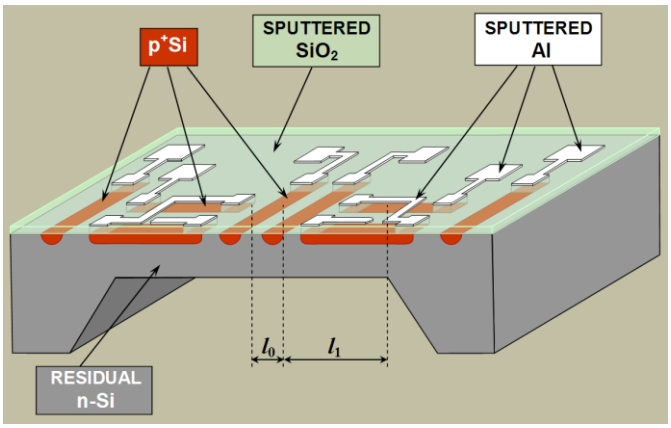

Fig. 2. Cross section of the P-type structure.

B. *Analytical model of transient response*

The thermal time constant (τ) of the sensors was calculated using expressions derived in [4, 7] which were modified by taking into account the pressure and temperature dependence of gas thermal conductivity. Influence of gas pressure was taken into account using relations presented in [6], while the temperature dependence of the thermal conductivity of the specific gas was calculated using data given in [3].

We assume that the sensor is mounted in a housing so that the distance between the upper side of the sensor and the housing cap is d_u and the distance between the bottom side of the membrane and the housing base is d_b. Taking into account the influence of both pressure and temperature, the thermal conductivity of the gas inside the housing can be calculated using the following relation:

$$\lambda_{gas}(p,T)=\left(\frac{1}{\lambda_{hp}(T)}+\frac{1}{\gamma_{lp}(T)p}\left(d_u^{-1}+d_b^{-1}\right)\right)^{-1}. \quad (1)$$

Parameters λ_{hp} and γ_{lp} are characteristic for the high and the low pressure region, respectively. The temperature dependence of the parameter λ_{hp} is described by relation given in [3]

$$\lambda_{hp}[mW/(Km)]=A\cdot(T/1000)^2+B\cdot(T/1000)+C, \quad (2)$$

where T is temperature in Kelvins [K], while A, B and C are constant coefficients.

At lower pressures, the dominant parameter is γ_{lp} which can be determined using relation given in [8]

$$\gamma_{lp}(T)=\frac{c}{3}\sqrt{\frac{8M}{\pi k_B T}}, \quad (3)$$

where $k_B = 1.38 \cdot 10^{-23}$ J/K is Boltzmann's constant, c is the specific heat capacity, M is the molecular weight and T is the ambient temperature.

The model presented in this work is based on the analytical model with two zones described in detail in [4]. The characteristic dimensions (l_0 and l_1) of each rectangular zone $j = \{0, 1\}$ of the two-zone model are marked in Figure 2. The length of the first zone, l_0, is constant and for the specific design equals 0.18 mm. The length of the second zone, l_1, depends on $d_{n\text{-}Si}$. In the case of anisotropic etching of Si (100) wafer with a nominal thickness of 380 μm the following relation is valid:

$$l_1 = 1620\ \mu m-\left(560\ \mu m+\frac{380\ \mu m-d_{n-Si}[\mu m]}{tg(54.7^o)}\right). \quad (4)$$

In general, in the zone "j" there are "n" layers of different materials "i" with their thickness d_i^j. In this model each multilayered zone is replaced with homogenous one characterized by equivalent parameters. In order to determine these parameters the coefficient of "coverage" k_i^j is introduced, defined as the ratio of the area covered by elements fabricated of material "i" to the area of the zone "j". Besides, for each zone the equivalent thickness is calculated using formula

$$d_e^j=\sum_{i=1}^{n}k_i^j d_i^j. \quad (5).$$

Based on this value, equivalent values of other parameters such as thermal conductivity (λ_e), thermal diffusivity (a_e), specific heat capacity (c_e) and density (ρ_e) can be calculated using general expression

$$\eta_e^j=\left(\sum_{i=1}^{n}k_i^j d_i^j \eta_i^j\right)\Big/ d_e^j, \quad (6)$$

where η_e^j represents any of the above listed parameters.

Using expressions derived in [4] the equation for the thermal time constant in the first order approximation can be deduced

$$\tau_1(p,T)=\frac{(l_0+l_1)^2}{\left(\frac{\pi}{2}\right)^2 a_e+\left(\frac{A_0(p,T)}{c_{e0}\rho_{e0}d_0}+\frac{A_1(p,T)}{c_{e1}\rho_{e1}d_1}\right)(l_0+l_1)}, \quad (7)$$

where:

- coefficient of total convective and radiative losses for the two zones is

$$A_j(p,T)=h_j(p,T)+4\sigma_B(\varepsilon_{ju}+\varepsilon_{jl})T^3,\ j=\{0,1\}, \quad (8)$$

where $\sigma_B = 5{,}67 \cdot 10^{-8}$ W/(m^{2}K^4) is Stefan-Boltzmann constant, while ε_{ju} and ε_{jl} are emissivities of the upper and the lower surface of the zone "*j*",

- convection coefficients for each zone are

$$h_j(p,T) = \lambda_{gas}(p,T)\left(d_u^{-1} + d_b^{-1}\right), \quad j = \{0,1\}, \qquad (9)$$

- equivalent thermal diffusivity, a_e, of the whole structure is determined based on the values of this parameter calculated for each zone using general formula (6), which are substituted in following expression

$$a_e = \frac{a_{e0} l_0 + a_{e1} l_1}{l_0 + l_1}. \qquad (10)$$

III. Results

Based on the analytical expressions derived in previous section, transient behaviour of the sensors was studied for an atmosphere of nitrogen (N_2), helium (He) and carbon dioxide (CO_2) at different ambient temperatures. The results obtained for nitrogen are a good approximation for air due to the dominant part of nitrogen in air composition.

The values of coefficients and parameters appearing in (2) and (3) are listed in Table I. The olecular weight of the chosen gases, *M*, is expressed in atomic mass units (1 u = $1.66 \cdot 10^{-27}$ kg).

TABLE I
VALUES OF COEFFICIENTS A, B AND C USED IN (2) FOR CALCULATION OF λ_{HP} AND PARAMETERS OF THE GASES OF INTEREST USED IN (3) FOR CALCULATION OF γ_{LP}

GAS	A	B	C	*c* [J/kgK]	*M* [u]
Nitrogen (N_2)	**-30**	**+90**	**+1.1**	**1041**	**28**
Helium (He)	**-100**	**+418**	**+37.6**	**5193**	**4**
Carbon dioxide (CO_2)	**-1**	**+83**	**-7.74**	**851**	**44**

Figure 3 presents a typical pressure dependence of gas thermal conductivity for all three chosen gases. Since helium has the highest thermal conductivity at atmospheric pressure, it undergoes the most prominent change with the change of pressure.

The transient response of the sensor is illustrated by its thermal time constant. Figure 4 shows the results of analytical simulation obtained for a P-type structure with $d_{n\text{-}Si}$ = 5 μm in nitrogen atmosphere for different ambient temperatures in the range (10 - 40) °C. It is obvious that ambient temperature does not have strong influence on the thermal time constant of the sensor. The influence of different gases on thermal time constant of the sensor was also studied.

Figure 5 shows simulation data obtained for a P-type structure with $d_{n\text{-}Si}$ = 3 μm and a structure with completely removed residual n-Si ($d_{n\text{-}Si}$ = 0 μm). The analysis was performed for the three chosen gases at an ambient temperature of 20 °C. The structure with completely removed residual n-Si is fabricated on a SOI wafer, which assures excellent thermal isolation. This effect in general improves the sensor performance. As illustrated in Fig. 5., at atmospheric pressure, the thermal time constant of the SOI structure is higher than in Si structure in nitrogen and carbon dioxide, while it remains the same for helium.

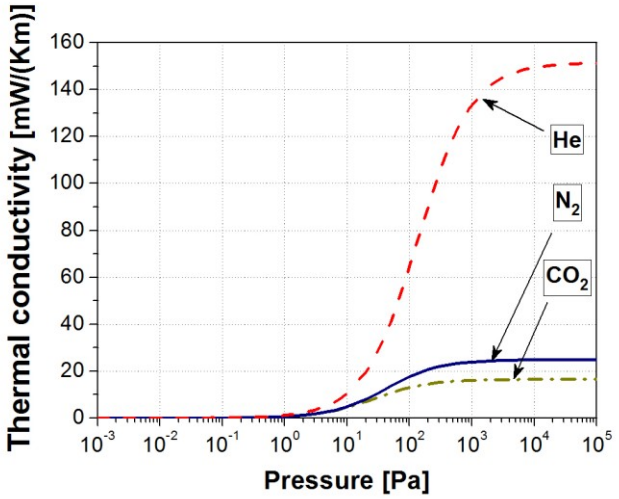

Fig. 3. Pressure dependence of thermal conductivity of helium, nitrogen and carbon dioxide at 20 °C.

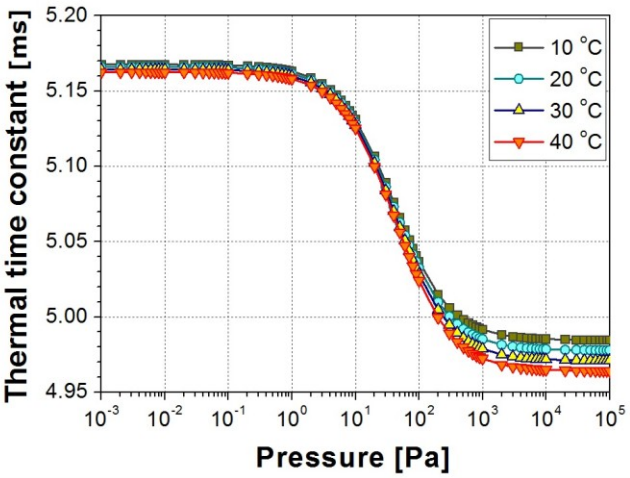

Fig. 4. Dependence of thermal time constant on nitrogen pressure at ambient temperatures (10, 20, 30, 40) °C. Simulations were obtained for P-type structure with $d_{n\text{-}Si}$ = 5 μm.

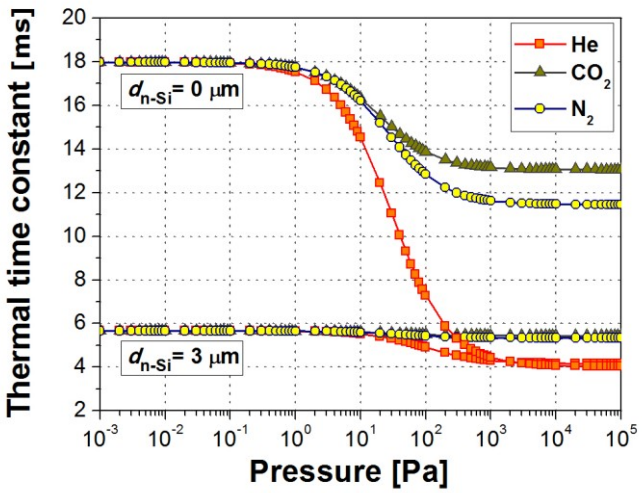

Fig. 5. Dependence of thermal time constant on pressures of He, CO_2 and N_2. Simulations were performed for P-type structures with $d_{n\text{-}Si}$ = 3 μm and $d_{n\text{-}Si}$ = 0 μm at ambient temperature of 20 °C.

Experiments were also conducted in order to measure the thermal time constant of the fabricated sensors. For this purpose, the heater of the sensors was connected to Hewlett-Packard 8002A Pulse Generator. Voltage pulses with 1.01 V amplitude, 100 ms width and a very long period were applied. The output signal was Seebeck voltage at one of the thermopiles. The thermopile voltage was stored using a Tektronix TDS3000B Digital Oscilloscope. As an illustration, measurement results obtained for A-type sensor with $d_{n\text{-}Si}$ = 10.5 μm are presented in Figure 6. Based on the analysis of the transient response of the sensors with different membrane thicknesses it was concluded that the thermal time constant assumes a value in the (4 – 5) ms range.

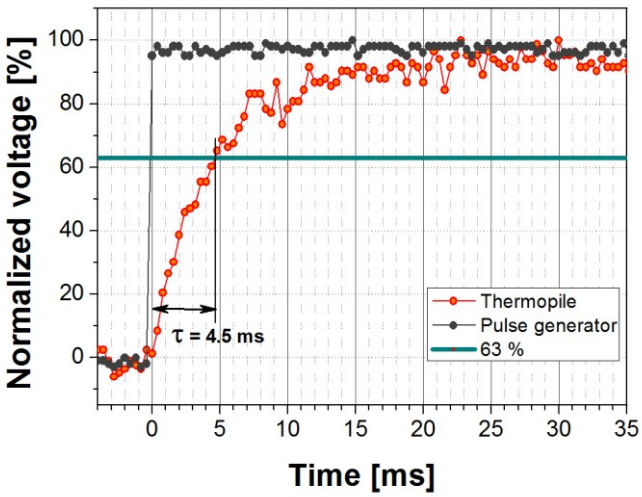

Fig. 6. Normalized input voltage generated with Pulse Generator and time response measured at one thermopile of A-type sensor with $d_{n\text{-}Si}$ = 10.5 μm.

IV. Conclusion

It can be concluded that ambient temperature does not exert a strong influence on the thermal time constant of the sensor. Simulation results are in good agreement with the experimental data obtained for sensors with various residual n-Si thicknesses. The influence of gas pressure and gas type on the thermal time constant is increasing with a decrease of residual n-Si thickness. Among gases of interest, helium has the strongest influence on the thermal time constant of thermopile sensors due to the fact that it is almost 5 times better thermal conductor compared with nitrogen and carbon dioxide.

The same conclusions are valid for A-type structures. Based on the results presented in [4], a somewhat lower value of the thermal time constant can be expected for the same thickness of residual n-Si in the case of A-type structures.

Gas type detection could be performed based on measurement of the thermal time constant of our multipurpose sensors. This analytical approach is generalized and flexible enough to be implemented for the analysis of the transient behaviour of thermopile-based sensors when used for different applications. Important conclusions regarding transient response can be deduced which should enable optimization of sensor structure for a specific application.

Acknowledgment

The authors would like to thank Mag. Sci. Dragan Tanasković from the ICTM-CMT for the photographs of the sensors.

References

[1] G. C. M. Meijer, A. W. Herwaarden, *Thermal Sensors*, IOP Publishing, Bristol, 1994.

[2] M. Bugnacki, J. Pyle, P. Emerald, ″A Micromachined Thermal Accelerometer for Motion, Inclination, and Vibration Measurement″, Sensors, June 2001, Available: http://archives.sensorsmag.com/articles/0601/98/index.htm.

[3] Xensor Integration, Available: http://www.xensor.nl/pdffiles/sheets/tcg3880.pdf .

[4] D. Randjelović, A. Petropoulos, G. Kaltsas, M. Stojanović, Ž. Lazić, Z. Djurić, M. Matić, "Multipurpose MEMS Thermal Sensor Based on Thermopiles", *Sens. Actuat. A-Phys*, vol. 141, pp. 404-413, 2008.

[5] D. Randjelović, Z. Djurić, A. Petropoulos, G. Kaltsas, Ž. Lazić, M. Popović, "Analytical modelling of thermopile based flow sensor and verification with experimental results", *Microelec. Eng.*, vol. 86, pp. 1293-1296, 2009.

[6] D. Randjelović, V. Jovanov, Ž. Lazić, Z. Djurić, M. Matić, "Vacuum MEMS Sensor Based on Thermopiles – Simple Model and Experimental Results", in *Proc. 26th Int. Conf. MIEL 2008*, Niš, Serbia, 2008, Vol 2, pp. 367-370.

[7] A. G. Kozlov, "Optimization of thin-film thermoelectric radiation sensor with comb thermoelectric transducer", *Sens. Actuators*, vol. 75, pp. 139-150, 1999.

[8] P. Eriksson, J. A. Anderson, G. Stemme, ″Thermal Characterization of the Surface Micromachined Silicon Nitride Membranes for Thermal Infrared Detectors″, *IEEE J. Microelectromech. Syst*., vol. 6, pp. 55-61, 1997.